^{13}C-NMR Relaxation in Three DNA Oligonucleotide Duplexes: Model-Free Analysis of Internal and Overall Motion†

Philip N. Borer,*,‡ Steven R. LaPlante,§ Anil Kumar,‖ Nilo Zanatta,⊥ Amy Martin, Anna Hakkinen,▽ and George C. Levy‡

Center for Science and Technology, Chemistry Department, Syracuse University, Syracuse, New York 13244-4100

Received November 24, 1993⊗

ABSTRACT: Natural-abundance ^{13}C-NMR spectra of [d(TCGCG)]$_2$ (**1**), [d(CGCGCG)]$_2$ (**2**), and [d(GGTATACC)]$_2$ (**3**) were measured at 90.6 MHz to obtain ^{13}C–^{1}H NOEs and T_1 relaxation times; relaxation data were also measured at 125.7 MHz for **1** and **2** and at 62.9 MHz for **1**. Analysis of the relaxation data was performed in the context of the "model-free" approach of Lipari and Szabo [Lipari, G., & Szabo, A. (1982) *J. Am. Chem. Soc. 104,* 4546–4559], leading to the following conclusions: (i) Optimized values for the overall correlation times of 0.9 ns for **1** and 1.4 ns for **2** are close to those predicted by light-scattering results on similar molecules [Eimer *et al.* (1990) *Biochemistry 29,* 799–811]. (ii) For the nonterminal residues, the "order parameter", S^2, is around 0.8 for the protonated base carbons and 0.6 for the sugar carbons, indicating less spatial restriction on the sugar carbons (in the model-free approach, the order parameter is 1 for a rigid body and 0 for a system with completely unrestricted internal motion). (iii) The order parameters for the terminal residues vary over a wide range with the smallest values around 0.2–0.3 for the HO–^{13}C5′ and the ^{13}C3′–OH; rational trends are seen in the variation of S^2 with chain position in the terminal residues. (iv) The analysis shows that the order parameters are accurate within 15%. (v) The "effective internal correlation time", τ_e, is very short for the sugar carbons (30–300 ps) and less well-defined, but probably also short, for the bases. (vi) The analysis indicates that most of the relaxation in DNA is accounted for by S^2 and that τ_e is so short that a good approximation to any relaxation property, P (e.g., T_1, T_2, ^{13}C–^{1}H NOE, ^{1}H–^{1}H cross-relaxation rate), is $P = S^2P_{rigid}$, where P_{rigid} is the value for the property in a system without internal motion (the analysis assumes the same isotropic overall motion for both the rigid and flexible bodies).

DNA is a highly flexible molecule, so a complete physical description *must* include the time scales and amplitudes of internal motion. This issue is receiving more attention in recent published studies of the "structures" of biopolymers determined by NMR methods, which are indeed "averaged structures". Nearly every study of the dynamical properties of DNA agrees that the motions are more restricted for the bases than the sugars, but the degree of site-specific variation deserves more careful examination.

The combination of NMR (Reid, 1987; Wagner, 1990; Fesik & Zuiderweg, 1990; Nirmala & Wagner, 1988; Kay *et al.*, 1989; Clore *et al.*, 1990a) with routine oligonucleotide synthesis makes it possible to ascertain the relationship of local structure and internal motion. The use of ^{13}C-NMR[1] relaxation parameters for dynamical analysis is attractive because the C–H bond distance is nearly constant at 1.09 Å. Thus, interpretation of the relaxation parameters reduces to analysis of ^{13}C–^{1}H vectors as a function of time. Models for this type of motion are much simpler to construct than those for ^{1}H–^{1}H vectors where the interproton distance may fluctuate substantially. Our group has examined several oligo-DNAs by ^{13}C-NMR, and, among other findings, we have shown that certain of the carbons near the sites of hydrogen-bond formation undergo unusual chemical shift effects (Borer *et al.*, 1984, 1988; LaPlante *et al.*, 1988a,b). For the sugar carbons, the effects of sequence and temperature on the ^{13}C chemical shifts appear to be closely related to the pseudorotational state of the furanose ring (LaPlante *et al.*, 1994).

The field of DNA dynamics has been highly controversial, partly due to the difficulty of generating meaningful physical models for overall and internal motion and also because the detailed motions of DNA in solution are certainly complex. However, the overall motion of molecules that are nearly spherical can be described by a single correlation time, thus removing one level of complexity. The overall motion of a B-DNA duplex should be fairly well approximated by considering it as a cylinder with a diameter of roughly 20 Å (larger if hydration layers move with the duplex) and length 3.4n Å, where n is the number of base pairs. Thus, molecules with 4–8 base pairs should be roughly spheroidal, including the pentamer, hexamer, and octamer duplexes analyzed in this work. Longer duplexes require a more sophisticated model

† This work was supported in part by National Institutes of Health Grants GM 32691, GM 35069, and RR 01317.

* Author to whom correspondence should be addressed.

‡ Chemistry Department, Syracuse University.

§ Present address: Biomega, Inc., 2100 rue Cunard Laval, Quebec, H7S 2G5 Canada.

‖ Present address: Department of Pharmaceutical Chemistry, University of California, 1034 Medical Sciences Building, San Francisco, CA 94143.

⊥ Present address: Departmento de Quimica, Universidade Federal de Santa Maria, 97100 Santa Maria-RS, Brazil.

▽ Present address: Department of Radiotherapy and Oncology, Helsinki University Central Hospital, SF-00290, Helsinki, Finland.

⊗ Abstract published in *Advance ACS Abstracts,* February 1, 1994.

[1] Abbreviations: ^{13}C, carbon-13; NMR, nuclear magnetic resonance; ^{1}H, proton; A, adenosine; T, thymidine; G, guanosine; C, cytidine; R, purine nucleoside; Y, pyrimidine nucleoside; ψ-state, a specific envelope or twist pseudorotational state of the furanose ring (Saenger, 1984). The oligonucleotides discussed in this paper have no terminal phosphates; therefore the IUPAC notation for oligomers is abbreviated by leaving out the phosphodiester linkage. Other nomenclature conventions are presented elsewhere (LaPlante *et al.*, 1994).

0006-2960/94/0433-2441$04.50/0

for overall motion since the correlation time for rotation about the helix axis will be shorter than for tumbling end over end.

MATERIALS AND METHODS

^{13}C T_1 and NOE Measurements. Samples of $[d(TCGCG)]_2$ (**1**), $[d(CGCGCG)]_2$ (**2**), and $[d(GGTATACC]_2$ (**3**) were prepared as described in the accompanying paper (LePlante et al., 1994). One-dimensional ^{13}C-NMR spectra were acquired at 125.78 MHz (General Electric GN-500), 90.56 MHz (Bruker WM-360), and 62.90 MHz (Cryomagnet Systems CM-250). All spectra reported here were obtained in 2 mL of 0.1 M NaCl, 0.01 M PO_4^{3-} pH 7.0, 0.1 mM EDTA, 0.01% NaN_3, 10% D_2O/90% H_2O in 10-mm NMR tubes at 30 °C. The strand concentration C_s = 20 mM for **1** (10 mM in duplex), 14 mM for **2** (7 mM in duplex), and 22 mM for **3** (11 mM in duplex). Spectra were obtained by one-dimensional direct detection of the natural-abundance ^{13}C signals, using the fast inversion–recovery technique for measuring T_1 and gated decoupling for measuring ^{13}C–^1H NOE. Details of the measurements are given by Zanatta *et al.* (1987) and Zanatta (1985). Assignments were from high-resolution 1D ^{13}C *vs* temperature profiles (Borer *et al.*, 1984; Zanatta *et al.*, 1987; LaPlante *et al.*, 1988a,b, 1994), confirmed by comparison to 2D ^1H–^{13}C HMQC spectra of $[d(TAGCGCTA)]_2$ (Ashcroft *et al.*, 1989; LaPlante *et al.*, 1994).

Theory. Lipari and Szabo (1982) put forward a "model-free" approach that, partially because it submerges the issue of a detailed motional mechanism, has been used widely to describe broad features of the dynamics of DNA (Williamson & Boxer, 1989; Eimer *et al.*, 1990; Withka *et al.*, 1991; Koning *et al.*, 1991) and proteins (Dellwo & Wand, 1989; Kay *et al.*, 1989; Clore *et al.*, 1990b). The simplest form of the model-free approach assumes isotropic overall motion with a correlation time, τ_m, and partitions the internal motions between two parameters. The first is a generalized order parameter, S^2, that describes the spatial restriction on the motion (S^2 = 1 for a rigid part of a molecule and decreases toward zero for parts that are less well-ordered). The second parameter, τ_e, has the appearance of a correlation time for internal motion but in fact depends on the spatial nature of the motion as well as the internal diffusive rates. A specific motional model is needed for a complete interpretation, but a short τ_e generally correlates with fast processes, while larger values indicate slower rates of internal motion. In this paper the collective term "derived parameters" is used for τ_m, S^2, and τ_e, or for the closely related set τ_m, θ_w, and τ_w, from the diffusion-in-a-cone model (Lipari & Szabo, 1981). The term "relaxation parameters" is used for the measured quantities (in this work, ^{13}C–^1H T_1, T_2, NOE, and ^1H–^1H cross-relaxation rate, σ_{ij}).

In our ^{13}C studies on DNA oligomer duplexes (*vide infra*) we find that S^2 is approximately 0.8 for the base carbons and 0.6 for the sugars. Williamson & Boxer (1989) studied a small DNA hairpin which had S^2 = 0.5–0.6 for ^{13}C-labeled thymine bases in the unpaired regions and either 0.8 or 0.7 (it is not clear from the text) for the base-paired cytosines in the stem (from σ_{56}). In proteins, S^2 averages *ca.* 0.7 for the $^{13}C\alpha$ in cyclosporin (Dellwo & Wand, 1989); in staphylococcal nuclease it is *ca.* 0.8–0.9 for the $^{13}C\alpha$ and most of the amide ^{15}N nuclei (McCain *et al.*, 1988; Kay *et al.*, 1989). In contrast, freely moving side chain carbons have $S^2 \leq 0.15$ (*e.g.*, Henry *et al.*, 1986).

The spectral density at a particular frequency, ω, is easily calculated in the model-free context (Lipari & Szabo, 1982) and takes an especially simple form for isotropic overall motion with a correlation time τ_m:

$$J(\omega) = (2/5)(S^2\tau_m/(1 + (\omega\tau_m)^2) + (1 - S^2)\tau/(1 + (\omega\tau)^2)) \quad (1)$$

where $1/\tau = 1/\tau_m + 1/\tau_e$. More complex spectral densities have been derived that include additional correlation times and order parameters for nonisotropic tumbling and/or more than one class of internal motion (Lipari & Szabo, 1982; Clore *et al.*, 1990a).

Computer calculations using eq 1 allow for the possibility that the internal motions may be comparable to τ_m. However, eq 1 is easier to grasp when $\tau_m \gg \tau_e$ and $\omega\tau_e \ll 1$. The first condition causes $\tau \cong \tau_e$, and the second, $1 + (\omega\tau)^2 \cong 1$. Thus, when the internal motions are much faster than overall reorientation and in "extreme narrowing" for τ_e, eq 1 becomes

$$J(\omega) \cong (2/5)(S^2\tau_m/(1 + (\omega\tau_m)^2) + (1 - S^2)\tau_e) \quad (2)$$

It is now easily seen that the first term on the right has S^2 modifying the effect of the overall correlation time with no contribution from the rate of internal motion, while the second reflects the influence of the rate of internal motion. Equations for σ_{ij}, T_1, T_2, and NOE can be cast in a similar form [*e.g.*, see Lipari and Szabo (1982)], where the first term involves S^2 modifying the effect of τ_m and the second of τ_e on relaxation. It should be emphasized that the simplified form in eq 2 is useful mainly in mentally relating the spectral density to simple motional concepts. However, the exact equation is used to calculate $J(\omega)$ in the computer program Moldyn (Craik *et al.*, 1983) which was used in our analysis. Therefore, when the program is used to optimize the derived parameters from the measured relaxation data (or to produce three-dimensional manifolds—see Discussion), the $\tau_m \gg \tau_e$ and $\omega\tau_e \ll 1$ approximations are not made. It should be noted that Moldyn also includes (i) spectral densities for other motional models, (ii) general expressions for calculating the relaxation parameters, and (iii) a nonlinear least squares subroutine for optimizing the derived parameters. The program has been modified recently to include the effect of chemical shift anisotropy (CSA) in the calculations and to calculate σ_{ij} (program available on request).

Dellwo and Wand (1989) point out that the order parameter is easily related to the amplitude of motion in the diffusion-in-a-cone model, without any dependence on τ_e. This is one instance of how it is possible to interpret S^2 values in a specific motional model.

Search Procedure to Escape False Minima. A particular measured relaxation parameter may be consistent with several sets of derived parameters, so a nonlinear optimization routine such as that in Moldyn may find different solutions depending on the allowed range and initial guess at the derived parameters. This will be more apparent in the Discussion of the T_1 and NOE manifolds in Figures 5 and 6. We limited the ranges to $0.1 < S^2 < 1.0$, $0.8 < \tau_m < 20$ ns, and $0.001 < \tau_e < 2$ ns, with eight initial guesses in all combinations of S^2 = 0.8 or 0.2, τ_m = 1 or 10 ns, and τ_e = 0.05 or 1.5 ns.

RESULTS

^{13}C-Relaxation in Three DNA Oligomers. Table 1 gives the T_1 and NOE values measured at three field strengths for the ^{13}CH and $^{13}CH_2$ in **1** (which has "dangling" unpaired T-residues at the 5′-ends), and Table 2 reports the results at two fields for **2**. Duplex **3** was studied only at 90.6 MHz; the

Table 1: Mean Relaxation Parameters for [d(TCGCG)]$_2$[a]

	62.9 MHz		90.6 MHz		125.8 MHz	
carbon[b]	NT_1	NOE	NT_1	NOE	NT_1	NOE
T1,6	0.12	1.56	0.15	1.52	0.23	1.33
C2,6	0.14	1.03	0.16	1.51	0.19	1.46
G3,8	0.14	1.32	0.13	1.35	0.18	1.24
C4,6	0.10	1.98	0.13	1.58	0.17	1.26
G5,8	0.19	1.01	0.21	1.52	0.28	1.48
T1,5′	0.33	1.23	0.40	1.20	0.46	1.54
T1,4′	c	c	0.30	1.87	0.41	1.70
T1,3′	0.24	1.72	0.25	1.63	0.39	1.56
T1,2′	0.18	1.65	0.22	1.78	0.39	1.43
T1,1′	c	c	0.22	1.87	0.41	1.67
C2,3′	0.20	1.94	0.22	1.60	0.32	1.58
C2,1′	c	c	0.22	1.52	0.28	1.60
G3,5′	0.13	1.91	0.18	1.72	0.25	1.41
G3,4′	c	c	0.21	1.52	0.27	1.55
G3,3′	0.15	1.79	0.21	1.69	0.25	1.30
C4,5′	0.19	1.89	0.23	1.58	0.28	1.65
C4,4′	0.14	2.03	0.18	1.58	0.32	1.63
C4,3′	0.18	1.94	0.22	1.78	0.30	1.62
G5,5′	0.15	1.56	0.19	1.56	0.25	1.49
G5,4′	c	c	0.22	1.69	0.32	1.54
G5,3′	0.27	1.91	0.31	1.59	0.43	1.58
G5,2′	0.26	2.23	0.32	1.61	0.43	1.50

[a] The N in NT_1 corresponds to the number of attached protons; N = 2 for ^{13}C5′ and ^{13}C2′, otherwise N = 1. The means reported in the table were for three independent determinations at 62.9 MHz, four at 90.56 MHz, and two at 125.78 MHz. Standard deviations about the mean were ±12% in the T_1 values and ±8% in NOE at 90.6 MHz. All measurements were made at 30 °C, C_s = 20 mM (10 mM in duplex), 0.1 M NaCl, pH 7.0 in 10% D_2O/90% H_2O. [b] The designation of the ^{13}C atoms indicates the nature of the base, T, C, or G, followed by the chain position numbered from the free 5′-OH end, followed by a comma and the atom number within each residue. [c] These resonances overlapped others at 62.9 MHz such that reliable measurements could not be made. The resonances for ten carbons overlapped others at all field strengths; these are not included in the table (C2,5, C4,5, C2,2′, C2,4′, C2,5′, G3,2′, G3,1′, C4,2′, C4,1′, and G5,1′).

Table 2: Mean Relaxation Parameters for [d(CGCGCG)]$_2$[a]

	90.6 MHz		125.8 MHz	
carbon[b]	NT_1	NOE	NT_1	NOE
G(2,4),8	0.15	1.27	0.17	1.24
C(3,5),6	0.14	1.31	0.13	1.15
G6,8	0.17	1.28	0.21	1.27
C1,5′	0.38	1.92	0.38	1.25
C1,4′	0.29	1.59	0.39	1.56
C1,3′	0.27	1.54	0.45	1.72
C1,1′	0.29	1.54	0.40	1.60
G(2,4),5′	0.22	1.33	0.32	1.38
G(2,4),4′	0.22	1.56	0.28	1.41
G(2,4),3′	0.16	1.68	0.25	1.35
G(2,4),1′	0.20	1.54	0.28	1.33
C(3,5),5′	0.20	1.44	0.30	1.35
C(3,5),4′	0.20	1.48	0.29	1.60
C(3,5),3′	0.28	1.48	0.32	1.39
C(3,5),2′	0.28	1.47	0.34	1.54
C(3,5),1′	0.21	1.41	0.30	1.42
G6,5′	0.20	1.32	0.22	1.40
G6,4′	0.27	1.73	0.28	1.42
G6,3′	0.33	1.39	0.45	1.49
G6,2′	0.38	1.64	0.48	1.53
G6,1′	0.20	1.53	0.28	1.50

[a] The N in NT_1 corresponds to the number of attached protons; N_2 = 2 for ^{13}C5′ and ^{13}C2′, otherwise N = 1. The means reported in the table were for three independent determinations of NOE and two of T_1 at 90.56 MHz, whereas single measurements were made at 125.78 MHz. Standard deviations about the mean were ±7% in the T_1 value and ±17% in NOE at 90.6 MHz. All measurements were made at 30 °C, C_s = 14 mM (7 mM in duplex), 0.1 M NaCl, pH 7.0 in 10% D_2O/90% H_2O.[b] The designation of the ^{13}C atoms indicates the nature of the base, C or G, followed by the chain position numbered from the free 5′-OH end, followed by a comma and the atom number within each residue. Parentheses indicate resonances that overlapped in the same carbon class for nonterminal residues, *e.g.*, G(2,4),1′. When different carbon classes overlapped, they were not included in the analysis (*viz.*, C1,2′, G2,2′, and G4,2′).

results are reported in Table 3. For **1** the only entries are for nonoverlapping resonances which have unambiguous assignments, whereas for **2** and **3**, entries are also kept for those carbons which could be identified as belonging to the same internal carbon class if they overlap only each other, *e.g.*, G2,2′ and G4,2′. Only 3 base and 8 sugar carbons had completely nonoverlapping signals in **3**.

Figure 1 shows the magnetic field dependence of the averaged relaxation parameters for **1**. The general trend for this duplex, as well as for several other molecules we have studied, is toward an increase in T_1 and a decrease in NOE as the Larmor frequency, ν_0, increases. Note the consistent difference in these average NOE and T_1 values between the sugars and the bases and for nonterminal (NT) *vs* terminal (T) residues. The temperature at which half the duplexes dissociate to monomer strands $T_m \cong 50$ °C for **1** in our experiments, so it is partially a monomer strand (≤10%) under the conditions shown in Figure 1. The trends in the field strength dependence of T_1 and NOE are very similar for **2**, which has $T_m > 70$ °C, so the issue of partial duplex melting is probably not too important for the present interpretation (see Figure 3 and the T_1 and NOE data in Table 2). The degree of duplex melting can be gauged by examining Figures 2–6 in LaPlante *et al.* (1994).

DISCUSSION

Many people interpret measurements of relaxation times from a background knowledge of rigid isotropic motion. This leads directly to paradox in the case of internally flexible bipolymers, at least for molecules that tumble slowly. The next few paragraphs use our experiments with DNA dynamics as examples, but the conclusions are general and give insight into a broad range of applications in biopolymer relaxation work.

The decrease in NOE and increase in T_1 expressed in Figure 1 are the expected behavior for isotropic overall motion with no internal motion on the slow motion (right) side of the T_1 minimum (see Figure 2; *e.g.*, T_1 increases and NOE decreases with ν_0 at $\tau_m = 10^{-8.5}$). However, the rigid model is clearly inadequate for two reasons: (i) the NOE and T_1 values are different for the sugars *vs* bases and for NT *vs* T at each ν_0 and (ii) one would conclude from Figure 2 that the sugars are more restricted than the bases and the terminal residues more restricted than the nonterminal ones! This is certainly not in line with current understanding of DNA dynamics [*e.g.*, Kearns (1987)]. [To illustrate the second point, examine the 90.6-MHz T_1 curve at the right of Figure 2; a decrease in T_1, as shown from sugar to base in Figure 1, requires faster motion (to the left along the τ_m axis) for the bases.]

The resolution to the paradox lies in properly accounting for the effects of overall and internal motion. Here the Lipari and Szabo (1982) "model-free" approach is used to analyze the NMR relaxation parameters. For **1** and **2**, isotropic reorientation is a good approximation to the overall motion (Eimer *et al.*, 1990). It is also a good approximation to ignore all but the dipole–dipole relaxation mechanism for the sugar carbons (which are sp^3). However, the CSA mechanism

Table 3: Relaxation Parameters for $[d(GGTATACC)]_2$[a]

	90.6 MHz		derived parameters[c]	
carbon[b]	NT_1	NOE	S^2	τ_e (ps)
G2,8	0.16	1.39	0.77	340
A(4,6),2	0.15	1.52	0.47	68
A(4,6),8	0.16	1.37	0.79	320
C7,6	0.16	1.31	0.84	250
C8,6	0.16	1.44	0.71	380
av base	0.16	1.41	0.74	350
			0.73	210[d]
G1,5′	0.30	1.94	0.34	110
G1,4′	0.28	1.41	0.57	48
T3,3′	0.22	1.55	0.60	110
T5,3′	0.30	1.88	0.36	106
T(3,5),2′	0.27	1.54	0.54	78
C7,5′	0.25	1.61	0.55	110
C7,3′	0.24	1.45	0.65	85
C8,3′	0.48	1.94	0.22	54
C8,2′	0.46	1.78	0.27	46
av sugar	0.26	1.61	0.53	91
			0.67	170[e]

[a] The N in NT_1 corresponds to the number of attached protons; N = 2 for ^{13}C5′ and ^{13}C2′, otherwise N = 1. All measurements were made at 30 °C, C_s = 22 mM (11 mM in duplex), 0.1 M NaCl, pH 7.0 in 10% D_2O/90% H_2O. [b] The designation of the ^{13}C atoms indicates the nature of the base, A, T, C, or G, followed by the chain position numbered from the free 5′-OH end, followed by a comma and the atom number within each residue. Parentheses indicate resonances that overlapped in the same carbon class for nonterminal residues, *e.g.*, T(3,5),2′. When different carbon classes overlapped, they were not included in the analysis (the majority of carbons in this molecule). [c] The derived parameters were optimized using τ_m = 3.2 ns, the light-scattering value for the octamer duplex, $[d(CG)_4]_2$, in Eimer *et al.* (1990). [d] In this case τ_m was freely optimized, resulting in a value of 2.8 ns. [e] In this case τ_m was freely optimized, resulting in a value of 4.7 ns.

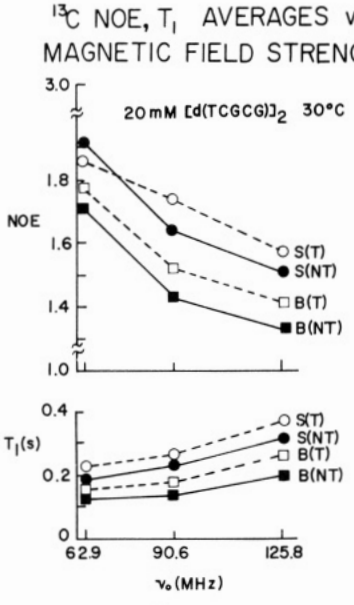

FIGURE 1: Mean values of ^{13}C T_1 (bottom) and NOE (top) as a function of spectrometer frequency. The labels S and B distinguish sugar and base carbons, while T and NT denote terminal and nonterminal residues, respectively. Strand concentrations were 20 mM (10 mM duplex), and measurements were made at 30 °C.

becomes important for the base carbons (sp^2), especially at higher field strengths, so we used the value $\Delta\sigma$ = 185 ppm determined by Williamson and Boxer (1988) for C6 of thymine as a CSA correction for each of the base carbons. Values of τ_m = 1.1 ns for **1** and 1.5 ns for **2** at 30 °C can be approximated from the depolarized dynamic light scattering (DDLS)

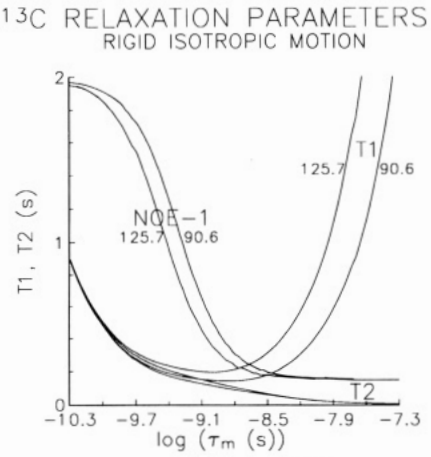

FIGURE 2: Dependence of ^{13}C T_1, T_2, and NOE on correlation time (τ_m) for rigid isotropic motion at two spectrometer frequencies. The rate of motion increases toward the left.

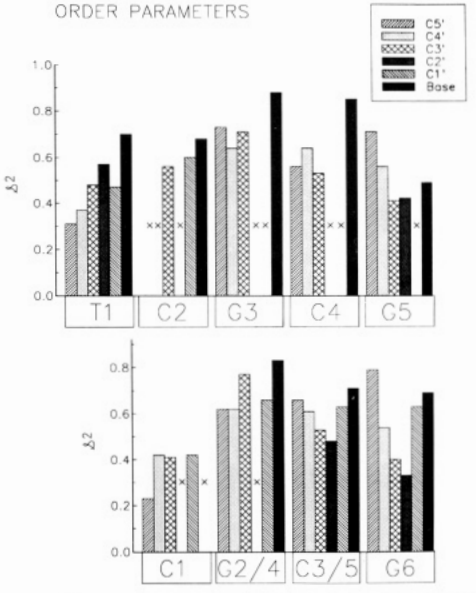

FIGURE 3: Order parameters (S^2, Lipari & Szabo, 1982; "model-free" approach) derived from the ^{13}C T_1 and NOE data in Table 1 for $[d(T1C2G3C4G5)]_2$ (top) and in Table 2 for $[d(C1G2C3G4C5G6)]_2$ (bottom). Bars indicate carbons on each residue: C5′, C4′, C3′, C2′, C1′, base, from left to right. Missing bars indicated by "×" are for carbon resonances which overlapped others or had ambiguous assignments; when the overlap in $[d(CGCGCG)]_2$ occurred only between resonances in the same carbon class on the nonterminal G2/G4 or C3/C5 residues, the order parameters derived from these combined signals are included. The uncertainty in the order parameters is estimated at ~15%.

measurements shown in the Eimer *et al.* (1990) paper (their Figure 1 shows the temperature dependence of a hexamer-length hairpin, and Figure 3, the chain length dependence). In the section on error analysis, we show that our ^{13}C-relaxation measurements are consistent with the DDLS values (see below).

Using the DDLS-fixed values of τ_m and the relaxation parameter measurements, S^2 and τ_e were optimized using the Moldyn program. The results for S^2 within each residue are shown in Figure 3 for each sugar and base carbon; here "×" designates those carbons excluded due to overlap or ambiguous assignment; only the 125.8- and 90.6-MHz data were used.

The most striking results are that the order parameters are largest for the base carbons (average 0.79 for NT) and that those for the sugar carbons vary widely (average 0.62 for NT). The τ_e values range from 20 to 150 ps for the sugar

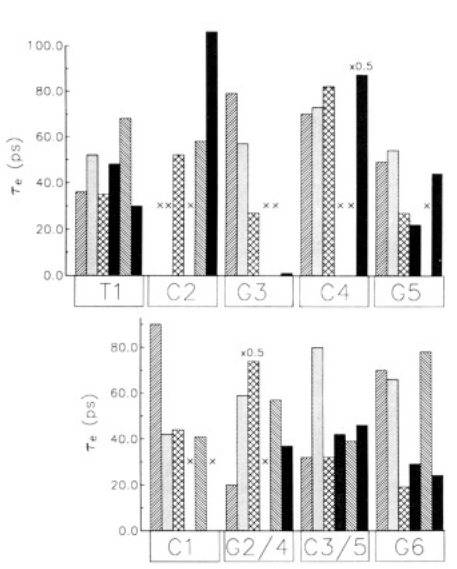

FIGURE 4: Approximate values for the model-free internal correlation times (τ_e, Lipari & Szabo, 1982). The uncertainties are as large as 100 ps for the sugar carbons and even larger for those carbons with $S^2 > 0.8$. The designations of the bars and panels is the same as in Figure 3.

carbons and are short but wildly varying for the bases (Figure 4). An obvious question relates to the confidence that can be placed in these derived parameters. This will be considered in the next section and has been the subject of a Monte Carlo analysis of the errors (Yu, J., Blumenthal, D., & Borer, P., unpublished results). It can be briefly stated here that the individual S^2 values are accurate within *ca.* 15%. The τ_e values are much less well-defined by the experimental data; the analysis indicates that they are in the range of 30–300 ps, have uncertainties as large as 100 ps for the sugar carbons, and are probably not to be believed for most of the bases or any carbon that has $S^2 > 0.8$.

The data in Figure 3 show several fascinating trends in S^2 beyond the difference in bases and sugars. (i) The data are arranged in the order 5′–4′–3′–2′–1′–B in each residue, so it is easy to see the stairstep increase in S^2 for T1 of **1** moving from the free HO–C5′ along the chain 5′–4′–3′. The reversed stairstep is seen at the other end of the chain in G5 going 5′–4′–3′ to the end at the free C3′–OH. The same trend with nearly identical values of S^2 is seen at G6 of **2** as in G5 of **1**; the free HO–C5′ at C1 of **2** also has a very low order parameter, $S^2 \cong 0.2$. Similarly small order parameters are derived for the terminal HO–C5′ and C3′–OH of **3** (see Table 3, column 4, for G1,5′ and C8,3′). (ii) In comparing the first two molecules, the order parameters for the NT G sugars are similar to each other (average = 0.69 and 0.67) and are somewhat larger than those for the NT C sugars (average = 0.57 and 0.60; averages taken over C5′,C4′,C3′ because C2′,-C1′ are usually missing in **1** due to overlap). (iii) Only C3′ is resolved at every residue of **1**, and its crosshatched bar in Figure 3 increases steadily from both ends toward the middle, suggesting that G3 is the most tightly constrained residue in this small duplex. (iv) There appears to be no large degree of internal motion at C2′, contradicting results with longer DNA oligomers where only averaged relaxation properties could be measured (Levy *et al.*, 1983). (v) The T1 base in **1** is only a little less constrained than the internal bases, suggesting it is quite strongly stacked on the base-paired core, even more so than the 3′-terminal (base-paired) G5.

NMR analyses of the ^{1}H–^{1}H coupling constants of DNA oligomer duplexes commonly find that the purine residues are more conformationally pure, whereas the sugars attached to pyrimidines exist in a mixture of sugar puckers, usually 10–30% less of the S-family of conformers, especially in duplexes with alternating purine–pyrimidine sequences (*e.g.*, Rinkel *et al.*, 1987; Rinkel & Altona, 1987; Schmitz *et al.*, 1990, 1992, 1993; Wang, 1991; LaPlante *et al.*, 1994). The increased sugar motion apparent for these pyrimidine residues (see point ii above) is probably associated with the increased degree of conformational exchange between S and N forms, although the decrease in order parameter is only *ca.* 0.1 on the average. This contrasts with the sugar motions available in paired, terminal residues, where S^2 can decrease by 0.2–0.4 compared with nonterminal residues.

Even at natural abundance using 1D direct detection we have been able to observe features of the relative freedom of motion of oligonucleotide segments. Although some of the trends in the previous three paragraphs were expected, that in itself provides an important check on the validity of this, the first report of the use of *site-specific* ^{13}C-relaxation measurements in DNA sugars and bases. The similarity between the results for the two molecules argues that the order parameters presented here, as well as their trends, truly reflect sequence and chain position effects on internal motion. Beyond that, it is now possible to quantify the relative extent of disorder in bases *vs.* sugars, the relative extent of disorder in terminal *vs* nonterminal residues, and the range of variation to be expected in alternating G–C paired segments of DNA.

Future studies using ^{13}C-isotopic enrichment, and ^{1}H-detected ^{1}H–^{13}C 2D correlation techniques will have much greater sensitivity than those in the present report. 2D and 3D NMR experiments also dramatically reduce the severity of peak overlap. Using these newer methods, we can confidently expect to differentiate the relative mobilities in duplexes, loops, and drug/DNA complexes in a *site-specific* manner, with enough sensitivity in the measurements to distinguish subtle mobility differences.

Although they are not well-determined by our measurements, the very short τ_e values derived from the analysis suggest that the last term in eq 2 can be safely ignored in evaluating the effect of internal motion on ^{1}H–^{1}H NOE measurements. Thus, an approach where cross-relaxation rates are corrected by an order parameter should be quite successful. Koning *et al.* (1991) took this approach, where they analyzed molecular dynamics trajectories to obtain approximate values of S^2. They suggest that S^2 varies from 0.6 to 0.9 for interproton vectors, with the smallest values involving sugar protons. They further find a small improvement in the *R* factors and restraint energies when their order parameter corrections are applied in structural refinement of a DNA octanucleotide duplex. It should be cautioned that there is not a simple equivalence between S^2 for a ^{1}H–^{13}C vector and that for a ^{1}H–^{1}H vector. Perhaps one use of the ^{13}C-derived parameters will be to adjust the force fields in molecular dynamics calculations to reproduce the carbon relaxation parameters. Then an analysis such as that followed by Koning *et al.* may produce more reliable order parameters for the interproton vectors.

Analysis of Errors in the Determination of τ_m, S^2, and τ_e. It is difficult to determine the errors in the parameters derived from a nonlinear optimization. However, it is possible to distinguish which parameters will, or will not, be well-determined by examining graphs of the interdependence of the derived parameters. With two correlation times and an amplitude it is impossible to visualize the behavior of a T_1 or

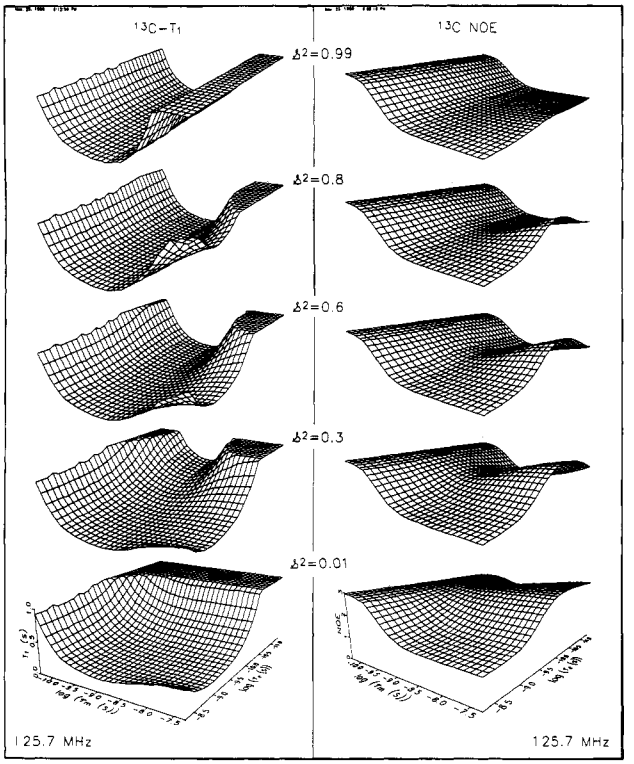

FIGURE 5: Manifolds showing the dependence of ^{13}C T_1 (left panels) and NOE (right panels) on the model-free parameters: τ_m (left/right), τ_e (front/back), and S^2 (top/bottom). See the bottom panels for the scales, which cover the ranges 50 ps $\leq \tau_m \leq$ 50 ns and 5 ps $\leq \tau_e \leq$ 5 ns. Faster motion occurs toward the left side and back of the plots. Highly restricted internal motion is characterized by the top and very free motion by the bottom panels. The manifolds can be thought of as the convolution of the familiar profile for T_1 *vs* τ_m (see Figure 2) with the same shape along τ_e (see, for example, S^2 = 0.6); a similar convolution of NOE profiles is also apparent (*e.g.*, see S^2 = 0.01). This emphasizes a rarely stated assumption of the model-free "model", *viz.*, that there is no coupling of overall and internal motion. The manifolds are calculated for isotropic overall motion at ν_0 = 125.7 MHz assuming only dipole–dipole relaxation. Values of $T_1 > 1$ s are shown as flat regions in the grid plots.

NOE manifold in five dimensions (*e.g.*, T_1, τ_m, S^2, τ_e, and ν_0). A four-dimensional sense of the dipole–dipole ^{13}C–^1H manifolds can be gained from Figure 5, which shows T_1 (left) and NOE (right) with the order parameter decreasing from top to bottom as noted in the figure (ν_0 = 125.7 MHz); this region represents the correlation time domain relevant to oligo-DNA dynamics (see Figure 5, bottom left panel, for the time scales which cover 3 orders of magnitude). Fortunately, the manifolds have similar shapes at other magnetic field strengths, so it is possible to understand the effect of the fifth dimension (ν_0) as well, using contour plots at a fixed value of S^2 (see Figure 6). The top panels of Figure 6 correspond to S^2 = 0.6, the second pair of manifolds in Figure 5; there is only a shift in the positions of the T_1 minima and NOE saddle points upon changing ν_0.

As S^2 approaches 1 (the top manifolds in Figure 5), one sees rigid isotropic behavior, as expected. However, it is clear that significant internal motion leads to considerable variation in the relaxation parameters. It is also clear that the shapes of the manifolds depend strongly on S^2. Furthermore, it can be seen that *nearly any value of* τ_e *fits* T_1 *and NOE when* S^2 *is large*, especially for values of τ_m less than or near the T_1 minimum. However, when S^2 = 0.6, the field dependence is very important in defining τ_e for the τ_m = 1–2-ns values that were found for **1** and **2**. Here, the simultaneous fit to T_1 and NOE to two or more fields constrains τ_e to a fairly narrow

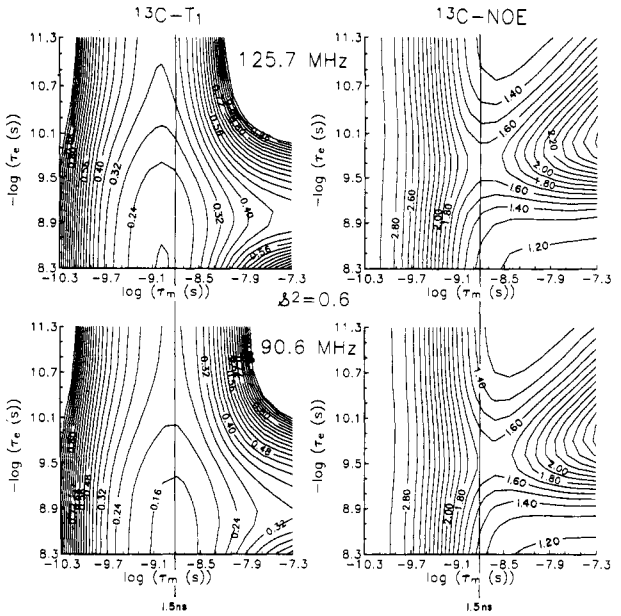

FIGURE 6: Contour plots for ^{13}C T_1 (left) and NOE (right) drawn at S^2 = 0.6; δ_0 = 125.7 and 90.6 MHz for the top and bottom panels, respectively. A vertical line indicates τ_m = 1.5 ns. The other details are the same as in Figure 5.

Table 4: Search Optima for Model-Free Dynamical Parameters in [d(TCGCG)]$_2$ and [d(CGCGCG)]$_2$

[d(TCGCG)]$_2$[a]	ν_0 used	τ_m (ns)	S^2	τ_e (ps)
av sugar, τ_m fixed	128/91/63	1.1[b]	0.64	72
av sugar, τ_m free	128/91/63	0.90	0.70	37
av sugar, τ_m free	128/91	0.86	0.70	33
av sugar, τ_m free	128/63	0.90	0.70	37
av sugar, τ_m free	91/63	0.90	0.70	52
av sugar, τ_m free	128	1.2	0.64	61
av sugar, τ_m free	91	1.2	0.60	100
av sugar, τ_m free	63	1.1	0.60	150
av base, τ_m free—1[c]	128/91/63	1.2	0.72	81
av base, τ_m free—2[c]	128/91/63	7	0.32	900
[d(CGCGCG)]$_2$[d]	ν_0 used	τ_m (ns)	S^2	τ_e (ps)
av sugar, τ_m fixed	128/91	1.5[b]	0.64	48
av sugar, τ_m free	128/91	1.4	0.64	44
av base, τ_m free—1[c]	128/91	1.3	0.84	1
av base, τ_m free—2[c]	128/91	20	0.19	1300

[a] 17 sugar ^{13}C in nonterminal residues, 16 base ^{13}C for 128/91/63 MHz; fewer when two or one ν_0 used (see Table 1). [b] τ_m value fixed to light-scattering prediction (Eimer *et al.*, 1990). [c] Two optima found. [d] 36 sugar ^{13}C on nonterminal residues, 15 base ^{13}C.

range. A Monte Carlo analysis of the errors in the derived parameters will be presented elsewhere (Yu, J., Blumenthal, D., and Borer, P., manuscript in preparation).

Search Strategy for Optimizing the Derived Parameters. The shapes of the T_1 and NOE manifolds presented in Figures 5 and 6 indicate that Moldyn optimizations can easily become trapped in false minima. For example, searches with initial guesses toward the right of the manifolds (large τ_m) may encounter extrema in moving back and forth in the τ_e direction. Therefore, we used a search strategy initialized with eight combinations of τ_m, S^2, and τ_e covering the range of reasonable values (see the end of Materials and Methods). For the present relaxation data, single optima were found for the sugar carbons, but two were encountered for the base carbons for each duplex. The results are summarized in Table 4 for averaged sugar carbons and averaged base carbons as well. It can be easily seen that values of τ_m and S^2 are highly self-consistent, no matter which field strengths are included in the analysis, and that fixing τ_m to give closest agreement with the DDLS value

causes no large variation in S^2 and τ_e in comparison to the free minimization. Of the two optima for the base carbons, one has τ_m very near that found for the sugars, lending further confidence to the determination of this value. The second optimum is at a much larger τ_m value and has an unrealistically low value for S^2 (less than for the sugars) and a slightly larger residual root-mean-square error, suggesting that it is not the global minimum.

The data in Table 4 for **1** also indicate the instability of the optimizations of τ_e. Determinations at a single field strength vary most widely, whereas the pairwise combinations are more self-consistent. This agrees with the previous discussion of Figure 5 and 6 that the simultaneous fit to T_1 and NOE at two fields constrains τ_e to a fairly narrow range as long as $S^2 < 0.8$. The derived parameters reported in Table 3 for **3** are less reliable because they come from single measurements of T_1 and NOE at a single field strength. However, from the preceding discussion, the similarities in the magnitudes of S^2 values to those of the other two molecules suggest that the comparisons between base *vs* sugar and T *vs* NT are reliable. The values derived for A(4,6)2 and T5,3′ appear somewhat unusual (Table 3). However, in relaxation measurements at 13 °C (Zanatta, 1985; Zanatta *et al.*, 1987), there appear to be no unusual values of T_1 or NOE at these sites, so we think these are more likely due to measurement errors (the relaxation data reported for the other molecules are averages of two or more measurements). We have not attempted to reinterpret the 13 °C relaxation measurements due to the likelihood that the duplexes aggregate under these conditions (Eimer *et al.*, 1990), making it unlikely that overall isotropic motion can be assumed; likewise, any other model for overall motion would be suspect.

In summary, when the ^{13}C-relaxation data are used to optimize τ_m as well as S^2 and τ_e, it is found that the value of the order parameter changes very little. For **1**, the optimized $\tau_m = 0.9$ ns and for **2**, $\tau_m = 1.4$ ns, both within experimental error of the light-scattering results. Finally, when the 62.9-MHz relaxation data on **1** are included in the analysis, S^2 is identical for the averaged sugar data and never differs by more than 0.03 for any individual carbon from the result analyzing only the data at 90.6 and 125.8 MHz (data not shown). The self-consistency of these results suggests that the order parameters are well-determined by the data.

Experimental Information on DNA Dynamics from Other ^{13}C-Relaxation Measurements. Perhaps the most informative experimental observations on DNA oligomers in solution are reported in the Eimer *et al.* (1990) paper, which compares results from ^{1}H and ^{13}C relaxation measurements with depolarized dynamic light scattering (DDLS). The light-scattering technique is very sensitive to the overall reorientation of a DNA oligomer duplex. Hence, internal motions contribute very little to the measurements, while the shape, state of aggregation, and properties of the hydration layer are central factors. These workers compared the properties of the hairpin loop oligonucleotide

$$\begin{array}{l} \text{CGCG}^{\text{TT}} \\ \qquad\quad \text{G} \\ \text{GCGC}_{\text{TT}} \end{array}$$

with the octamer duplex $[d(CG)_4]_2$ and the dodecamer, $[d(CG)_6]_2$. The results are compared in Table 5.

Based on Stokes–Einstein–Debye (SED) plots of the temperature dependence of τ_{LS} for the hairpin, the molecule was shown to tumble as a spheroid with a diameter around 22 Å, and a correlation time for overall motion of 1.9 ± 0.2 ns. A similar analysis is consistent with the octamer and dodecamer duplexes tumbling as cylinders with a diameter of *ca.* 22 Å. The SED plots also show nonlinearity for the duplex data at low temperatures that is consistent with end-to-end aggregation. Significant aggregation occurs below 20 °C with a duplex concentration of 6 mM, but there was no evidence of aggregation for the 3 mM hairpin. The NMR correlation times (see Table 5) were calculated assuming rigid isotropic motion using estimates of σ_{56} from measurements of the NOE buildup at cytidine H5 upon irradiation of H6; τ_{NMR} is always substantially less than τ_{LS}, arguing that internal motion affects the correlation times as measured by NMR.

Table 5: NMR and Light-Scattering Results[a]

	diameter (Å)	τ_{LS} (ns)	τ_{NMR} (ns)
hairpin	21.5 ± 2	1.9 ± 0.2	1.4 ± 0.3
8-mer	22.5 ± 2	3.2 ± 0.2	1.6 ± 0.3
12-mer	21.5 ± 2	6.4 ± 0.3	3.0 ± 0.4

[a] Eimer *et al.* (1990); correlation times at 20 °C.

Experimental Information on DNA Dynamics from ^{2}H Line Shape Measurements in the Solid State. One of the most useful techniques for evaluating motional models is the measurement of ^{2}H line shapes in the solid state, where the application to DNA is the subject of a recent review (Alam & Drobny, 1991). Among other topics, the review summarizes a series of experiments by Drobny and co-workers on the dodecamer duplex $[d(CGCGAATTCGCG)]_2$ with specific ^{2}H labels at the thymine methyl (TMe-D), thymine-6 (T6-D), purine-8 (R8-D), deoxythymidine-5′,5″ (T5′/5″-D), or deoxyadenosine-2″ (A2″-D). The authors developed a comprehensive model for overall and internal motions that adequately fits the measurements with as many as six adjustable parameters for extensively hydrated samples. In "dry" powders and those equilibrated at relative humidity (RH) levels below 66% (about 4 waters per nucleotide), it appears that overall motion can be ignored, and two-parameter fits are practical. As RH increases, successful models include overall motion about the long axis of the helix, until at very high RH levels (gel-like samples with 15–70 waters per nucleotide) the authors produce reasonable models that also include librations perpendicular to the helix axis. The overall motions were each parameterized with a jump amplitude and jump rates in the kilohertz range.

The most successful models for internal motion summarized by Alam and Drobny (1991) used a four-site, "biaxial", libration which is characterized by two angles centered about the C–D bond (the model is for uncoupled motion in orthogonal planes). The librations are in the fast-exchange limit (rate constants $k_{ex} > 10^5$ Hz) producing an averaged quadrupole coupling constant (QCC_{eff}), with only the two amplitude parameters subject to adjustment. Given the exchange regime, the parameters for internal motion should be weighted toward those with the largest amplitudes, especially if $k_{ex} \cong 10^9$ Hz as suggested by the ^{13}C-derived parameters reported here [assuming $k_{ex} \cong [(2\pi\tau_e)^{-1}]$. The amplitudes for the internal motions of the bases appear to be in the range of 10° (from the TMe-D, T6-D, and R8-D studies), 10–15° for the furanose rings in the deoxyA residues (from A2″-D), and 15–20° for the C5′,5″–D vectors near the outer periphery of a B-family DNA helix (from T5′/5″-D). The biaxial librations cannot have exactly the same magnitudes because there is a slight asymmetry in the powder pattern line shape; however, when the RMS values are compared to θ_w, the half-angle for the C–D bond to diffuse freely in a cone (Lipari & Szabo, 1981),

θ_w, is *ca.* 20° for RMS angles near 10° and is over 30° for RMS angles near 20° [see Table IX in Alam and Drobny (1991)]. These values can be used to estimate order parameters $S^2 = 0.83$ for internal motions of the bases ($\theta_w = 20°$) and $S^2 = 0.65$ for the most freely diffusing parts of the sugars ($\theta_w = 30°$) using eq 7 in Dellwo and Wand (1989). Therefore, the solid-state work on the dodecamer duplex suggests that the internal motion is slightly more restricted at the base and sugar sites probed than for our solution studies on shorter duplexes, with the same trend as reported in our work ($S^2 \cong 0.8$ for the bases and $S^2 \cong 0.6$ for the sugar carbons).

There was concern expressed in the Alam and Drobny (1991) paper that "large amplitude motions [≫20° (biaxial libration model)] in the fast rate regime" do not occur at the sites deuterated and that this may be inconsistent with popular interpretations of pseudorotational interconversion in the furanose ring in DNA and RNA. The latter interpretations assume fast exchange to explain averaging of ^1H–^1H coupling constants (*e.g.*, Rinkel and Altona, 1987; Bax and Lerner, 1988) and ^{13}C chemical shifts (*e.g.*, Lankhorst *et al.*, 1983; LaPlante *et al.*, 1994). Duplex "melting" to the monomer strands can usually be accomplished between room temperature and 100 °C, so many solution studies have followed changes in coupling constants and chemical shifts as a function of temperature. For samples at concentrations below 1–2 mM, most resonances are sharp before, during, and after the melting transition (although there is broadening when the duplex–monomer strand exchange rates are comparable to the difference in chemical shift for a nucleus in the duplex and monomer strand). The simplest interpretation of such observations is that the chemical shifts and coupling constants change as averages over an equilibrium blend of conformers in fast exchange.

Before attempting to reconcile the seemingly conflicting results, it is necessary to discuss briefly the pseudorotational (ψ) model [see Saenger (1984) for a full description]. The model classifies the furanose ring-puckered states into 10 "envelope" (E) forms as well as 10 "twist" forms and a continuum of intermediate microstates at higher energies. The E forms have four atoms lying in nearly the same plane, with the fifth either on the same side of this plane as C5′ (*endo*) or the opposite (*exo*). Some of the ψ-states can be simply interconverted, although relatively large concerted changes may be required in several torsional angles. Some other ψ-states are widely separated in the "pseudorotational cycle", in which case sequential passage through other ψ-states is required. The largest change in the ring atom torsional angles from a planar five-membered ring is a quantity called the maximum amplitude of pseudorotation, Φ_m, which is ∼35–40°. Calculations indicate that low energy barriers (0.5–5 kcal/mol; Saenger, 1984) separate the ψ-states commonly found in X-ray crystal structures of B-family DNA (S forms) from those usually found in A-family DNA and RNA (N forms). The highly populated ψ-states for the S forms have an easily measured $J_{H1'-H2'} \cong 7$–10 Hz, while $J_{H1'-H2'} \leq 2$ Hz for the N forms; more precise characterization of the ψ-states requires measurement of several three-bond coupling constants (Rinkel & Altona, 1987). The S forms are often carelessly described as 2′-*endo*, although that is only one of the distinct ψ-states usually found in crystals of B-family DNA; likewise, the N forms are often imprecisely described as 3′-*endo* conformers. During interconversion between S and N states many of the torsional angles have excursions as large as $2\Phi_m$ because the rings may pass through several ψ-states (at the very least they must pass through the O4′-*endo* state).

Six explanations are now presented that may reconcile the differences in interpretation of the solution and solid-state results.

First, in regard to the minor differences in S^2 between the solid-state results and the ^{13}C relaxation measurements on shorter DNA molecules reported here and in Eimer *et al.* (1990), the short helixes are more likely to have larger amplitude motions due to partial strand melting, especially near the helix-terminal residues (Tinoco et al., 1973).

Second, there is the possibility that mechanisms other than simple local motions may contribute to the relaxation. Schurr and Fujimoto (1988) and Schurr *et al.* (1989) in studies of the fluorescence depolarization anisotropy of ethidium intercalated into DNA reported that microsecond-scale bending and torsional motions contribute to NMR relaxation. This work was developed for DNA with hundreds of base pairs, so it is less likely that large-scale concerted motions occur in short oligomer duplexes. The same work showed that only small-angle librations occur in the base motions in concurrence with our results and the solid-state studies. As noted earlier, we have ignored CSA contributions to the internal motions of the sp^3 sugar carbons, an approximation that may be less valid at the higher field strengths. We have also approximated the T_1 relaxation times for methylene carbons (C2′ and C5′) as twice the measured value, assuming the relaxation contribution from the two protons occurs independently.

Third, there can be no model-independent relationship between Φ_m and S^2, QCC_{eff}, or even θ_w. In other words, the populations and rates of exchange between the various ψ-states will determine the characteristics of the libration of a C–H or C–D vector with respect to the magnetic field direction. Equating $2\Phi_m$ with an expected amplitude of internal motion of any bond is probably a mistake because concerted changes in torsional angles are required to jump from one ψ-state to another. These changes are certainly accompanied by changes in the exocyclic torsional angles as well. For the bases to remain relatively static, these concerted changes in torsional angles may compensate to reduce the librational amplitudes of the C–H or C–D vectors.

Fourth, in the study of $[d(CGCGAATTCGCG)]_2$, the dA residues strongly favor the S forms [93% and 94% according to Bax and Lerner (1988)]. Perhaps the librations involved in the pseudorotational equilibrium for these residues is particularly unfavorable toward averaging QCC_{eff} for the C–D vectors at the labeled dA2″-D sites. It would be especially interesting to measure the deuterium line shapes for sugars specifically labeled at some of the residues predicted to be in the 75–80% S range (Bax & Lerner, 1988).

Fifth, there are probably substantial differences between oligomer duplexes packed in a dry powder in comparison to duplexes tumbling freely in solution. Even when powders/gels are extensively hydrated, there are interduplex interactions that are absent at low concentration in solution, often including end-to-end stacking of duplexes. The indeterminate nature of these aggregates makes it very difficult to model the overall motion.

Sixth, analysis of the deuterium line shapes in highly hydrated powders may be predisposed toward models for internal motion developed for the dry and 66% RH powders, where overall motion is highly restricted. For the dry and 66% RH powders, two-parameter fits successfully model the line shapes, and even single-parameter fits are fairly good. The progression of parameters introduced to fit the line shapes for highly hydrated samples is logical. However, when many more adjustable parameters are required, perhaps another

choice of amplitudes for internal motion and rates and amplitudes for overall motion might produce satisfactory fits to the line shapes.

Experimental Information on DNA Dynamics from Measurements of ^{1}H–^{1}H Cross-Relaxation Rates. Some solution measurements have analyzed ^{1}H–^{1}H relaxation rates where the interproton distance is fixed. This was mentioned in connection with the Eimer *et al.* (1990) and Williamson and Boxer (1989) work discussed earlier in this section. In addition, Reid *et al.* (1989) suggested that the bases and sugars in DNA duplexes have the same correlation times, based on measurements of the ratio $\sigma_{2'2''}/\sigma_{56}$ in [d(CGCGAATTCGCG)]$_2$ using 2D-NOE spectra measured with very short mixing times. Their experimental evidence is that the initial buildup rate for several H2′–H2″ crosspeaks is 5.6–7.6 times faster than the H5–H6 buildup and that theoretically the ratio should be 6.97 for a rigid body using the standard H2′–H2″ and H5–H6 distances. (Actually, the uncertainties in the interproton distances allow the ratio to be in the range 6.2–7.5.)

There are two concerns regarding the Reid *et al.* (1989) interpretation of identical correlation times and a serious experimental problem in making the measurement. First, Withka *et al.* (1990) point out that an unhydrated dodecamer will not tumble isotropically; therefore the ratio of the σ_{ij} will be quite different from 6.97 in a rigid body because the base and sugar H–H vectors point in very different directions with respect to the helix axis. This criticism is less significant if the (unknown) geometry of hydration allows nearly isotropic motion for the duplex. Second, simple calculations using the approximate relation for the cross-relaxation rate

$$\sigma_{ij} = (\gamma_H^4 h^2/10 r_{ij}^6)[S^2\tau_m + (1 - S^2)\tau_e] \qquad (3)$$

show that there are many combinations of S^2 in the 0.6–0.9 range and τ_e in the 1–300-ps range that produce $\sigma_{2'2''}/\sigma_{56}$ near or above the experimental lower limit of 5.6 in the Reid *et al.* measurements. The experimental problem lies in the difficulty of suppressing zero-quantum (ZQ) coherences at the very short mixing times required to determine the initial slopes of the NOE buildup curves. This is especially a problem for crosspeaks near the diagonal, such as the H2′–H2″, where the suppression is not very efficient under the best of circumstances (Rance *et al.*, 1985). This is usually accomplished by a random "jiggling" of the mixing time, which cannot be done at 10–30-ms mixing times without disturbing the measurement since the jiggling time would have to be a substantial fraction of the mixing time. As a consequence of these concerns about the interpretation and accuracy of the measurements reported by Reid *et al.* (1989) and our own ^{13}C relaxation measurements, we dispute their assertion that DNA sugars and bases have the same motional properties. However, we do agree that the sugar and base motions are not radically different, as suggested by some earlier studies (Clore & Gronenborn, 1984a,b).

Effect of Motion on Distances Derived from Interproton NOE Measurements. Internal motion is expected to have a rather small effect on interproton NOE-based distance determinations in DNA. This results from the dependence of σ_{ij} on the sixth power of distance and the linear dependence on effective correlation time. These points are emphasized in examining eq 3; note that for the $\tau_m > 2$ ns values typical of macromolecules, the $(1 - S^2)\tau_e$ term contributes 3% or less to the effective correlation time (the quantity in square brackets in eq 3) using the conclusion from our ^{13}C relaxation measurements that $S^2 > 0.6$ and $\tau_e < 100$ ps for most bond

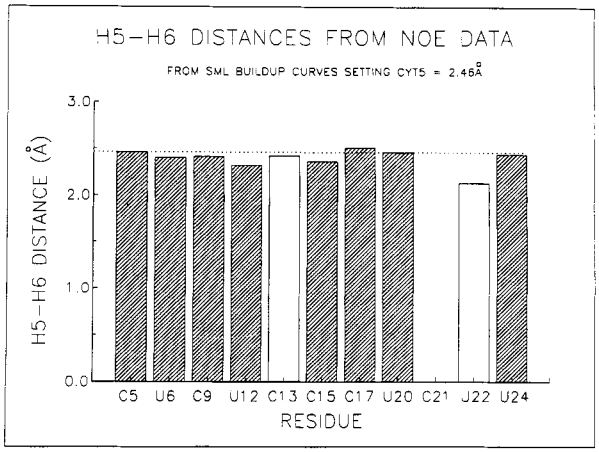

FIGURE 7: Interproton distances derived from buildup curves for the pyrimidine H5–H6 2D-NOE crosspeaks in the 24-mer RNA GGGACUGACGAUCACGCAGUCUAU referenced to 2.46 Å for the C5 residue (500-MHz spectrum, 1.7 mM, 30 °C). Crosshatched bars are for isolated crosspeaks, and open bars are for "factored" intensities (see text). The C21 crosspeak completely overlapped others, so it was not used for a distance calculation.

vectors. The sixth power *vs* linear dependence may not produce such a clear weighting toward distance effects in molecules that do not tumble isotropically and in situations where spin diffusion pathways cannot be distinguished in an unambiguous manner. The latter point has been illustrated by Withka *et al.* (1991) where the shapes of NOE buildup curves for [d(CGCGAATTCGCG)]$_2$ were shown to be affected by these factors.

However, in other work we have evidence that anisotropic tumbling and substantial variety in internal motion produce only minor effects on interproton distances derived from interproton NOE crosspeaks in an RNA 24-mer hairpin loop (Borer, P., *et al.*, in preparation). The buildup curves for 10 pyrimidine H5–H6 NOEs were measured, and using a cubic spline fit to determine the initial rate, the interproton distances were calculated by setting a reference distance of 2.46 Å for cytosine-5 (this base is located in the middle of a very stable, base-paired stem). The results are shown in Figure 7, with the shaded bars representing distances from isolated crosspeaks. The open bars result from integration of two nonoverlapping lobes of the AX crosspeaks in spectra deconvolved by the maximum likelihood method (Jeong *et al.*, 1992) and then multiplying the integral by 2 to estimate the total volume. The worst deviation for the isolated peaks is 0.14 Å, while for the less well-determined "factored" peaks, the worst deviation is 0.3 Å. Each of these distances is adequate for 3D structure determination. Note that U24 is an unpaired residue at the 3′-end of the chain and its furanose ring is about a 50:50 N:S pseudorotational blend. Likewise, U12 and C13 are at the turn of the chain in the loop with both residues in >60% S forms. C9 and C15 are N/S blends, while the others are almost completely in N states. If internal motion were to produce substantial effects on distances derived from NOE buildup rates, they should be apparent in this example (at least for distances <2.5 Å). It should now be much less surprising that the Reid *et al.* (1989) study found no substantial effect of differential base and sugar motion on proton cross-relaxation rates in a conformationally homogeneous DNA duplex.

As in the Withka *et al.* (1991) analysis there is some difference in the shapes of the H5–H6 buildup curves, especially at longer mixing times. Together these results indicate a need to ascertain the effects of motion in calculating

optimal interproton distances from complete relaxation analyses of NOE measurements at mixing times beyond the initial rate region (Borgias *et al.*, 1990; Schmitz *et al.*, 1990, 1992, 1993; Koning *et al.*, 1991). Even so, the determination that τ_e is very short in DNA implies that $S^2\tau_m \cong \tau_{eff}$ may be a sufficient approximation to correct for dynamical effects, at least in molecules that tumble isotropically. The RNA hairpin result in Figure 7 suggests that the most interesting focus of NMR relaxation analyses in nucleic acids may be the dynamical properties themselves rather than the effect of motion on distance determinations derived from interproton NOEs.

ACKNOWLEDGMENT

We are grateful to Prof. I. Pelczer for helpful discussions. The NMR1 software package was used to process spectra and calculate T_1 and NOE (Tripos Associates, St. Louis, MO); the *xy* plots, bar charts, and 3D manifold plots were prepared using the AXUM software package (Trimetrix Corp., Ravenna, WA).

REFERENCES

Alam, T. M., & Drobny, G. P. (1991) *Chem. Rev. 91*, 1545–1590.
Ashcroft, J., LaPlante, S. R., Borer, P. N., & Cowburn, D. (1989) *J. Am. Chem. Soc. 111*, 363.
Bax, A., & Lerner, L. (1988) *J. Magn. Reson. 79*, 429.
Borer, P. N., Zanatta, N., Holak, T. A., Levy, G. C., van Boom, J. H., & Wang, A. H.-J. (1984) *J. Biol. Struct. Dyn. 1*, 1373.
Borer, P. N., LaPlante, S. R., Zanatta, N., & Levy, G. C. (1988) *Nucleic Acids Res. 16*, 2323–2332.
Borgias, B. A., Gochin, M., Kerwood, D. J., & James, T. L. (1990) *Prog. Nucl. Magn. Reson. Spectrosc. 22*, 83.
Brandes, R., Vold, R. R., Kearns, D. R., & Rupprecht, A. (1990) *Biochemistry 29*, 1717–1721.
Clore, G. M., & Gronenborn, A. (1984a) *FEBS Lett. 172*, 219.
Clore, G. M., & Gronenborn, A. (1984b) *FEBS Lett. 172*, 117.
Clore, G. M., Szabo, A., Bax, A., Kay, L. E., Driscoll, P. C., & Gronenborn, A. M. (1990a) *J. Am. Chem. Soc. 112*, 4989–4991.
Clore, G. M., Driscoll, P. C., Wingfield, P. T., & Gronenborn, A. M. (1990b) *Biochemistry 29*, 7387–7401.
Craik, D. J., Kumar, A., & Levy, G. C. (1983) *J. Chem. Inf. Comput. Sci. 23*, 30–38.
Dellwo, M. J., & Wand, A. J. (1989) *J. Am. Chem. Soc. 111*, 4571–4578.
Eimer, W., Williamson, J. R., Boxer, S. G., & Pecora, R. (1990) *Biochemistry 29*, 799–811.
Fesik, S. W., & Zuiderweg, E. R. P. (1990) *Q. Rev. Biophys. 23*, 97–131.
Henry, G. D., Weiner, J. H., & Sykes, B. D. (1986) *Biochemistry 25*, 590–598.
Jeong, G.-w., Borer, P. N., Wang, S. S., & Levy, G. C. (1993) *J. Magn. Reson. Ser. A 103*, 123–134.
Kay, L. E., Torchia, D. A., & Bax, A. (1989) *Biochemistry 28*, 8972–8979.
Kearns, D. R. (1987) in *Two-Dimensional NMR Spectroscopy* (Croasmun, W. R., & Carlson, R. M. K., Eds.) p 301, VCH Publishers, New York.
Koning, T. M. G., Boelens, R., van der Marel, G. A., van Boom, J. H., & Kaptein, R. (1991) *Biochemistry 30*, 3787–3797.
Lankhorst, P. P., Erkelens, C., Haasnoot, C. A. G., & Altona, C. (1983) *Nucleic Acids Res. 11*, 7215.
LaPlante, S. R., Ashcroft, J., Cowburn, D., Levy, G. C., & Borer, P. N. (1988a) *J. Biomol. Struct. Dyn. 5*, 1089.
LaPlante, S. R., Boudreau, E. A., Zanatta, N., Levy, G. C., Borer, P. N., Ashcroft, J., & Cowburn, D. (1988b) *Biochemistry 27*, 7902.
LaPlante, S. R., Zanatta, N., Hakkinen, A., Wang, A. H.-J., & Borer, P. N. (1994) *Biochemistry*.
Levy, G. C., Craik, D. J., Kumar, A., & London, R. E. (1983) *Biopolymers 22*, 2703–2726.
Lipari, G., & Szabo, A. (1981) *J. Chem. Phys. 75*, 2971–2976.
Lipari, G., & Szabo, A. (1982) *J. Am. Chem. Soc. 104*, 4546–4559.
McCain, D., Ulrich, E. L., & Markley, J. L. (1988) *J. Magn. Reson. 80*, 296–305.
Nirmala, N. R., & Wagner, G. (1988) *J. Am. Chem. Soc. 110*, 7557.
Rance, M., Bodenhausen, G., Wagner, G., Wuthrich, G., Wuthrich, K., & Ernst, R. R. (1985) *J. Magn. Reson. 62*, 497.
Reid, B. R. (1987) *Q. Rev. Biophys. 20*, 1.
Reid, B. R., Banks, K., Flynn, P., & Nerdal, W. (1989) *Biochemistry 28*, 10001–10007.
Rinkel, L. J., & Altona, C. (1987) *J. Biomol. Struct. Dyn. 4*, 621.
Rinkel, L. J., van der Marel, G. A., van Boom, J. H., & Altona, C. (1987) *Eur. J. Biochem. 166*, 87.
Saenger, W. (1984) *Principles of Nucleic Acid Structure*, Springer-Verlag, New York.
Schmitz, U., Zon, G., & James, T. L. (1990) *Biochemistry 29*, 2537.
Schmitz, U., Kumar, A., & James, T. L. (1992) *J. Am. Chem. Soc. 114*, 10654.
Schmitz, U., Ulyanov, N. B., & James, T. L. (1993) *J. Biomol. Struct. Dyn. 10*, a171.
Schurr, J. M., & Fujimoto, B. S. (1988) *Biopolymers 27*, 1543–1569.
Schurr, J. M., Fujimoto, B. S., Wu, P., & Song, L. (1989) in *Fluorescence Spectroscopy: Principles and Applications* (Lakowicz, J., Ed.) Plenum Press, New York.
Tinoco, I., Jr., Borer, P. N., Dengler, B., Levine, M. D., Uhlenbeck, O. C., Crothers, D. M., & Gralla, J. (1973) *Nature New Biol. 246*, 40–41.
Wagner, G. (1990) *Prog. NMR Spectrosc. 22*, 101–139.
Wang, Y.-Y. (1991) Ph.D. Thesis, Syracuse University.
Williamson, J. R., & Boxer, S. G. (1988) *Nucleic Acids Res. 16*, 1529–1540.
Williamson, J. R., & Boxer, S. G. (1989) *Biochemistry 28*, 2819–2831.
Withka, J. M., Swaminathan, S., & Bolton, P. H. (1990) *J. Magn. Reson. 89*, 386–390.
Withka, J. M., Swaminathan, S., Beveridge, D., & Bolton, P. H. (1991) *J. Am. Chem. Soc. 113*, 5041–5049.
Zanatta, N. (1985) Ph.D. Thesis, Syracuse University.
Zanatta, N., Borer, P. N., & Levy, G. C. (1987) *Recent Advances in Organic NMR Spectroscopy* (Lambert, J., & Rittner, R., Eds.) pp 89–110, Norell Press, Landisville, PA.